Development of Spatial Distribution Patterns by Biofilm Cells

Haagensen, Janus Anders Juul; Hansen, Susse Kirkelund; Bak Christensen, Bjarke; Pamp, Sünje Johanna; Molin, Søren

Published in:
Applied and Environmental Microbiology

Link to article, DOI:
10.1128/AEM.01614-15

Publication date:
2015

Document Version
Publisher's PDF, also known as Version of record

AEM
Journals.ASM.org

Development of Spatial Distribution Patterns by Biofilm Cells

Janus A. J. Haagensen,[a] Susse K. Hansen,[b] Bjarke B. Christensen,[c] Sünje J. Pamp,[d] Søren Molin[a,b]

Novo Nordisk Foundation Center for Biosustainability, Technical University of Denmark, Hørsholm, Denmark[a]; Department of Systems Biology, Technical University of Denmark, Lyngby, Denmark[b]; Department of Food Science, University of Copenhagen, Frederiksberg, Denmark[c]; National Food Institute, Technical University of Denmark, Lyngby, Denmark[d]

Confined spatial patterns of microbial distribution are prevalent in nature, such as in microbial mats, soil communities, and water stream biofilms. The symbiotic two-species consortium of *Pseudomonas putida* and *Acinetobacter* sp. strain C6, originally isolated from a creosote-polluted aquifer, has evolved a distinct spatial organization in the laboratory that is characterized by an increased fitness and productivity. In this consortium, *P. putida* is reliant on microcolonies formed by *Acinetobacter* sp. C6, to which it attaches. Here we describe the processes that lead to the microcolony pattern by *Acinetobacter* sp. C6. Ecological spatial pattern analyses revealed that the microcolonies were not entirely randomly distributed and instead were arranged in a uniform pattern. Detailed time-lapse confocal microscopy at the single-cell level demonstrated that the spatial pattern was the result of an intriguing self-organization: small multicellular clusters moved along the surface to fuse with one another to form microcolonies. This active distribution capability was dependent on environmental factors (carbon source and oxygen) and historical contingency (formation of phenotypic variants). The findings of this study are discussed in the context of species distribution patterns observed in macroecology, and we summarize observations about the processes involved in coadaptation between *P. putida* and *Acinetobacter* sp. C6. Our results contribute to an understanding of spatial species distribution patterns as they are observed in nature, as well as the ecology of engineered communities that have the potential for enhanced and sustainable bioprocessing capacity.

Microorganisms in nature are not entirely randomly distributed and often exhibit distinct patterns of spatial organization. Species distribution patterns are influenced by the species' inherent capabilities, environmental conditions, and historical contingencies (1). Microbial spatial organizations are evident in the environment (e.g., microbial mats, soil communities, and headwater stream biofilms) as well as in communities associated with humans and animals (e.g., tooth plaque, chronic wounds, and gutless worms) (2–7). The underlying evolutionary and developmental processes of these communities often remain elusive. Distinct spatial distribution patterns of cells are also observed in experimentally established biofilm communities, and particular processes of their evolution, metabolic capabilities, and tolerance toward antimicrobials have been revealed (8–12).

Acinetobacter sp. strain C6 and *Pseudomonas putida* are members of a natural microbial consortium that was isolated from a creosote-polluted aquifer in Denmark in the 1990s (13). Previous examinations of this two-species consortium provided insight into their spatial multicellular organization and underlying evolutionary and cometabolic processes (9–11). When they are cocultivated in laboratory flow chambers with aromatic compounds as carbon sources, they assemble in a systematic manner. (i) *Acinetobacter* sp. C6 forms microcolonies and metabolizes benzyl alcohol to benzoate. (ii) *P. putida* evolves genetic variants that have an increased ability to attach to *Acinetobacter* sp. C6 and form a mantle-like subpopulation over the top of the microcolonies. *P. putida* metabolizes benzoate produced by *Acinetobacter* sp. C6, as it is less effective at metabolizing benzyl alcohol. (iii) The two-species consortium exhibits increased stability and productivity compared to the individual strains or when its members are cultivated together in a chemostat environment (9–11). Hence, the spatial distribution of *Acinetobacter* sp. C6 determines the spatial distribution of *P. putida*, and microcolony formation is the fundamental initial step for the evolution of this symbiotic species interaction.

In this study, we analyzed the spatial ecology of *Acinetobacter* sp. C6 multicellular assemblages, and we describe the processes that lead to the microcolony pattern in space and time. We discovered that *Acinetobacter* sp. C6 exhibits a dynamic migration pattern: small multicellular clusters move along the surface in an apparently coordinated fashion and fuse to form uniformly arranged microcolonies. The spatial distribution pattern of microcolonies develops in response to the available carbon source and oxygen, leading to phenotypic variants that consistently emerge under these conditions. We conclude that the spatially organized two-species consortium of *Acinetobacter* sp. C6 and *P. putida* is the result of spatiotemporal coadaptation.

MATERIALS AND METHODS

Bacterial strains and cultivation. Bacterial strains used in this study are listed in Table 1. *Acinetobacter* sp. strain C6 (NCBI accession number Y11464.1) was originally isolated from a creosote-polluted aquifer in Fredensborg, Denmark (13). The strain has 98.3% 16S rRNA sequence similarity to *Acinetobacter johnsonii* type strain ATCC 17909 (NCBI accession

Received 14 May 2015 Accepted 19 June 2015
Accepted manuscript posted online 26 June 2015
Citation Haagensen JAJ, Hansen SK, Christensen BB, Pamp SJ, Molin S. 2015. Development of spatial distribution patterns by biofilm cells. Appl Environ Microbiol 81:6120–6128. doi:10.1128/AEM.01614-15.
Editor: M. Kivisaar
Address correspondence to Sünje J. Pamp, sjpa@food.dtu.dk.
Supplemental material for this article may be found at http://dx.doi.org/10.1128/AEM.01614-15.

doi:10.1128/AEM.01614-15

TABLE 1 Bacterial strains used in this study

Strain	Relevant characteristics	Reference
Acinetobacter sp. C6 (CKL01)	Natural isolate; *Gammaproteobacteria*; Strep^r; GenBank accession no. Y11464.1	11
JH07	*Acinetobacter* sp. C6; Gfp Strep^r Km^r	This study
JH08	*Acinetobacter* sp. C6; Rfp Strep^r Km^r	This study
JH102	*Acinetobacter* sp. C6 variant; Strep^r	This study
JH111	*Acinetobacter* sp. C6 variant; Gfp Strep^r Km^r	This study
JH114	*Acinetobacter* sp. C6 variant; Rfp Strep^r Km^r	This study

number Z93440.1) and 97.1% 16S rRNA sequence similarity to *Acinetobacter haemolyticus* type strain DSM6962 (NCBI accession number X81662.1). The phylogenetic relationships between *Acinetobacter* sp. C6 and 26 *Acinetobacter* type strains are presented in Fig. S1 in the supplemental material. For routine strain maintenance, *Acinetobacter* sp. C6 was cultivated on Luria broth (LB) plates containing 100 μg/ml of streptomycin as described previously (11). In biofilms, *Acinetobacter* sp. C6 was grown in FAB minimal medium [1 mM $MgCl_2$, 0.1 mM $CaCl_2$, 0.01 mM Fe-EDTA, 0.15 mM $(NH_4)SO_4$, 0.33 mM Na_2HPO_4, 0.2 mM KH_2PO_4, and 0.5 mM NaCl] (10) containing one or two of the following carbon sources: 0.5 mM benzyl alcohol (Merck, Darmstadt, Germany), 0.5 mM benzoate (Sigma Chemical Co., St. Louis, MO), 0.1 mM glucose (Sigma-Aldrich Co.), 0.1 mM citrate (Sigma-Aldrich Co.), or 50-times-diluted LB. Where required, antibiotics were added at final concentrations of 100 μg/ml of streptomycin and 25 μg/ml of kanamycin.

Fluorescently labeled *Acinetobacter* sp. strains JH07 and JH08 were constructed by biparental mating between *Acinetobacter* sp. C6 (CKL01) and SM1921, expressing green fluorescent protein (Gfp), and SM1923, expressing red fluorescent protein (Rfp), respectively, similarly to a previous description (14).

Biofilm variants were isolated from microcolonies of 3-day-old *Acinetobacter* sp. C6 biofilms grown on benzoate minimal media. Using a micromanipulator and microscope (Leica Lasertechnik GmbH, Heidelberg, Germany), cells were isolated from microcolonies, resuspended in 0.9% NaCl solution, and plated on LB agar with streptomycin. The colony morphology of these isolated variants had a wild-type phenotype. Individual randomly selected colonies were grown in LB medium with streptomycin and inoculated in the flow channels as described below, and their biofilm phenotypes were examined.

Flow chamber experiments. Biofilms were grown at 22°C in three-channel flow chambers with individual channel dimensions of 40 by 4 by 1 mm (length by width by height). The flow system was assembled and prepared as described previously (10, 15). The substratum consisted of a microscope glass coverslip (Knittel Gläser, Braunschweig, Germany). Each channel was supplied with a flow of 3 ml/h of FAB medium containing the appropriate carbon source (see above). *Acinetobacter* sp. C6 was grown for 18 h in LB medium and then diluted to an optical density (OD) of 0.5 in FAB medium containing the appropriate carbon source. Medium flow was paused, the flow channels were turned upside down, and 250 μl of the diluted cell suspension was carefully injected into each flow channel using a small sterile syringe. After 1 h of incubation, the flow channels were turned upright again, and the flow was resumed using a Watson Marlow 205S peristaltic pump (Watson Marlow Inc., Wilmington, MA). The flow velocity in the flow cells was 0.2 mm/s. In order to determine the spatial localization of single cells and biofilms that developed in the flow channels using confocal microscopy, either *Acinetobacter* sp. C6 was hybridized with a CY3-labeled probe as described previously (11, 16) or isogenic strains expressing Gfp or Rfp were used (see above).

To supply *Acinetobacter* sp. C6 with additional oxygen, the fact that silicone tubes have a high permeability to oxygen was exploited. The medium supporting the flow chamber was enriched with oxygen by placing 2 m of silicone tube connected to the inlet of the flow system into a flask with water that was constantly saturated with pure oxygen. In this way, the oxygen concentration increased 5-fold compared to standard conditions in the influx medium to the flow chamber (see Fig. S3b in the supplemental material). For measurement of oxygen concentrations, T-connectors were inserted before and after each flow channel. In this way, the concentration of oxygen could be measured at any time during the experiments using a Unisense OX500 microelectrode (Unisense, Aarhus, Denmark) connected to the ampere meter with a built-in polarization source, Unisense PA2000 (Unisense). Calibration and control experiments for measurements of oxygen concentrations were performed in water saturated with either air or nitrogen (zero point).

Microscopy and image analysis. All microscopic observations and image acquisitions were performed either on a Leica TCD4D confocal laser scanning microscope (Leica Lasertechnik GmbH, Heidelberg, Germany) or a Zeiss LSM510 confocal laser scanning microscope (Carl Zeiss, Jena, Germany), each equipped with an argon/krypton laser and detectors and filter sets for simultaneous monitoring of Gfp (excitation, 488 nm, and emission, 517 nm) and Rfp and CY3 (excitation, 543 nm, and emission, 565 nm). Images were obtained using 63×/1.4 Plan-APOChromat DIC, 40×/1.3 Plan-Neofluar oil, and 10×/0.3 Plan-Neofluar objectives. Multichannel simulated fluorescence projection (SFP) shadow projection images and vertical cross sections through the biofilm were generated using IMARIS software (Bitplane AG, Zürich, Switzerland). Time series experiments were performed on a Zeiss LSM510 microscope, and video sequences were produced using Jasc software (Animation Shop).

Statistical analysis. For the quantification of *Acinetobacter* sp. C6 growing on different carbon sources (benzyl alcohol, benzoate, glucose, and citrate), two independent biofilm experiments were performed, acquiring at least 9 image stacks per channel (two channels per experiment), carbon source, and time point combination on days 1, 2, and 3. The sampling sites (i.e., sites from which image stacks were acquired) were selected randomly in the flow channels using a 40×/1.3 Plan-Neofluar oil objective. Images were analyzed using COMSTAT software and ImageJ (17, 18). The ecological micrococolony distribution pattern was analyzed according to the method of Clark and Evans (19) based on 200 distances measured using ImageJ. R is defined as the ratio of the observed nearest-neighbor distance in comparison to the expected nearest-neighbor distance at a given density of individuals, with σrE as the standard error and c as the standard variate (19). Values of R lower than 1 are indicative of a clumped spatial distribution, a value of 1 indicates a random distribution, and values greater than 1 are indicative of a uniform spatial distribution pattern. Standard variate values greater than 1.96 or lower than −1.96 represent the 5% level of significance, and values greater than 2.58 or lower than −2.58 represent the 1% level of significance (19).

RESULTS

Spatial abundance distribution by *Acinetobacter* sp. C6. In the symbiotic two-species consortium of *P. putida* and *Acinetobacter* sp. C6, *P. putida* is dependent on microcolonies formed by *Acinetobacter* sp. C6, to which it attaches (Fig. 1a) (9). To unravel the processes that lead to the formation of microcolonies by *Acinetobacter* sp. C6, we studied their development in the absence of *P. putida*. When grown on benzoate for 3 days, *Acinetobacter* sp. C6 forms microcolonies with a diameter of 16.10 μm (±1.97) on average (Fig. 1b and c). The microcolonies were relatively evenly spaced, with a nearest-neighbor distance of 13.04 μm (±3.19) on average and a resulting diameter/distance ratio of 1:0.8 (Fig. 1d). The microcolony density was homogenous, with 15.78 (±1.52) microcolonies per 10^4 μm^2 (Fig. 1e). Ecological spatial pattern analysis according to the method of Clark and Evans (19) revealed that *Acinetobacter* sp. C6 exhibited the tendency to a uniform microcolony distribution pattern, with an R value of 1.42 (σrE = 0.68; c = −7.95) (Fig. 1f). If one interprets the microcolony pattern at the level of single cells, then the pattern is the result of groups of cells that coexist in niches. The abundance of cells is

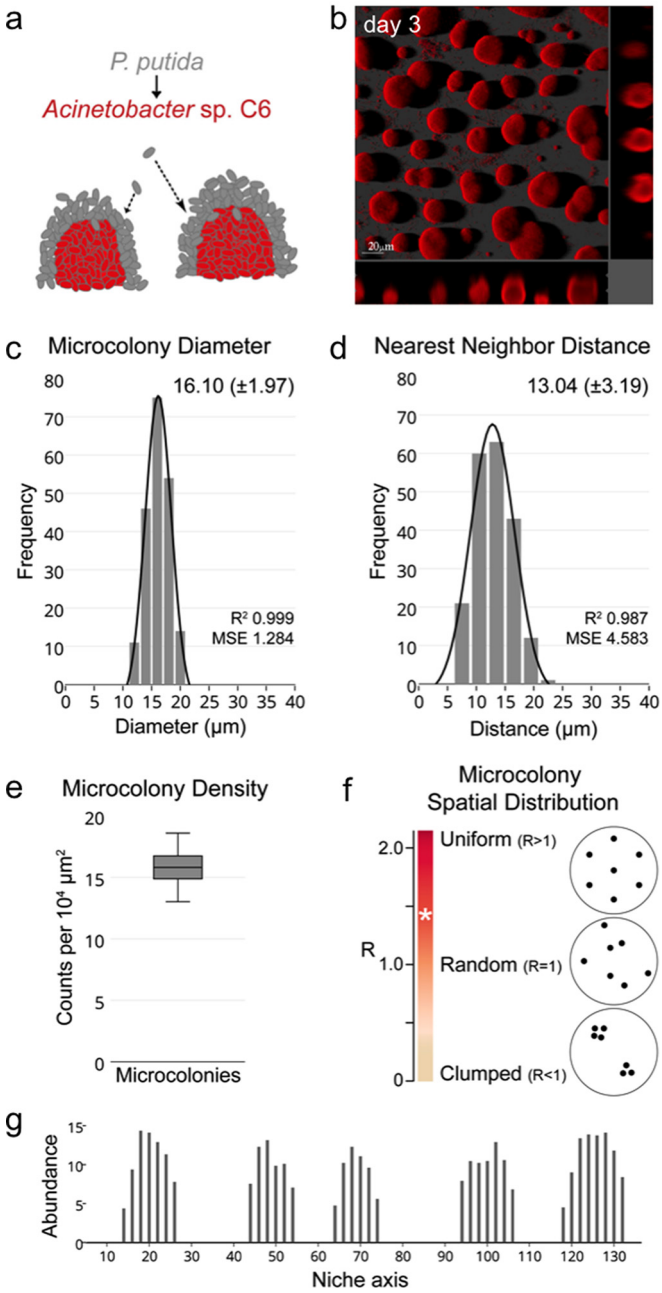

FIG 1 Spatial abundance distribution by *Acinetobacter* sp. C6. (a) In the symbiotic two-species consortium, *P. putida* attaches to microcolonies formed by *Acinetobacter* sp. C6 (9, 11, 20). (b) Confocal laser scanning micrograph of *Acinetobacter* sp. C6 cultivated for 3 days in minimal medium with benzoate as the sole carbon and energy source. (c) Diameters at day 3 of 200 *Acinetobacter* sp. C6 microcolonies grown in the presence of benzoate. MSE, mean squared error. (d) Nearest-neighbor distances at day 3 from 200 *Acinetobacter* sp. C6 microcolonies grown in the presence of benzoate. (e) Density at day 3 of *Acinetobacter* sp. C6 microcolonies grown in the presence of benzoate. (f) Spatial distribution of microcolonies determined according to the method of Clark and Evans (19). *Acinetobacter* sp. C6 exhibited an R value of 1.42 (white asterisk). R values of <1, 1, and >1 denote clumped, random, and uniform spatial distribution patterns, respectively. (g) Schematic representation of *Acinetobacter* sp. C6 abundance along a representative spatial niche axis at the substratum after 3 days of cultivation in benzoate minimal medium. The height of microcolonies was measured every 2 μm along the vertical section of a 140-μm niche axis in the x-plane.

highest within the microcolonies and lowest (or even absent) in the space between microcolonies along a niche axis (Fig. 1g).

Spatial abundance distribution is dependent on environmental factors. To examine the impact of environmental factors on *Acinetobacter* sp. C6 microcolony pattern formation, we exposed the strain to different carbon sources, namely, citrate, glucose, benzoate, and benzyl alcohol. While in the initial phase (day 1) of biofilm development a random spatial distribution of single cells along the niche axes was observed under any conditions, the ultimate three-dimensional spatial abundance distribution (day 3) was dependent on the carbon source (see Fig. S2 in the supplemental material). In the presence of glucose and citrate, *Acineto-*

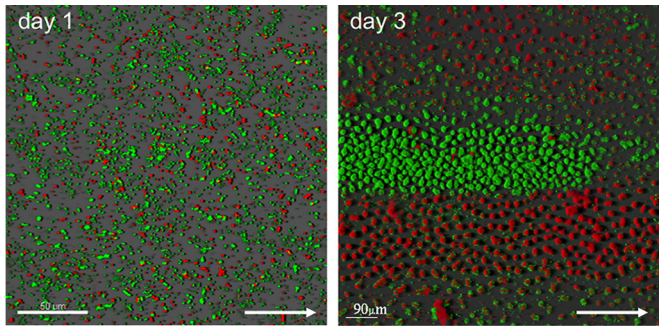

FIG 2 Microcolonies of the same origin colocalize in distinct niche space. A 1:1 mixture of isogenic strains of *Acinetobacter* sp. C6 tagged with Gfp (green) and Rfp (red) were established in flow chambers in benzoate minimal medium, and the distribution of green and red fluorescent cells was monitored by confocal laser scanning microscopy (CLSM). CLSM micrograph of the initial distribution of cells at day 1 (left) and CLSM micrograph of the final distribution of microcolonies at day 3 (right). The arrow points in the direction of the flow chamber inlet.

bacter sp. C6 covered the niche space homogenously, and the abundance of cells was equally high across niche axes. In contrast, spatial abundance distribution in the presence of benzyl alcohol was similar to the microcolony pattern observed with benzoate (see Fig. S2). Thus, in the presence of aromates, *Acinetobacter* sp. C6 occupies the niche in the form of groups of cells and leaves void, unoccupied niche space in between groups. Our previous analyses suggested that the oxygen concentration was low around *Acinetobacter* sp. C6 microcolonies (20). Hence, we reasoned that cells avoided this space due to the limited oxygen concentration. This hypothesis was supported by the fact that when the oxygen concentration was increased, the previously void space in between microcolonies was now occupied with *Acinetobacter* sp. C6 cells (see Fig. S3 in the supplemental material). Therefore, microcolony pattern formation by *Acinetobacter* sp. C6 is influenced by environmental factors that include carbon source and oxygen.

Microcolonies of the same origin colocalize in distinct niche space. To further explore the mechanism of microcolony formation by *Acinetobacter* sp. C6, we examined if microcolonies developed as a result of either clonal growth or cell aggregation. We used a double-tagging strategy as described previously (21–23). After mixing Gfp- and Rfp-tagged *Acinetobacter* sp. C6 cells in a ratio of 1:1 and introducing them into flow cells, we monitored their distribution in space and time. On day 1, the surface showed a random distribution of green and red cells (Fig. 2). After 3 days, however, a clear distribution of confined areas composed of either green or red microcolonies was observed (Fig. 2). At the borders of the confined areas, two-color-coded microcolonies were observed. This suggests that microcolonies were formed by a combination of clonal growth and cell aggregation. The shape of a respective distinct monochromatic area as a linear patch in space along the flow direction suggested that the microcolonies within a linear patch might originate from the same source located upstream in the flow channel.

Primary colony formation and emergence of cell clusters. The hypothesis of a common source located upstream was supported by results from time-lapse recordings of the early stages of *Acinetobacter* sp. C6 biofilm development. Individual large colonies appeared, growing up from loci on the lawn of cells and expanding in size during the first day of biofilm development (Fig. 3a; see also Movie S1 in the supplemental material). The large colonies expanded further by a combination of dissolution, release of cells that reattached downstream in flow direction, proliferation, and thereby formation of small cell clusters in flow direction by day 2 (Fig. 3b; see also Movie S2). Interestingly, whereas only a fraction of ancestral *Acinetobacter* cell colonies (i.e., primary colonies) developed in the early biofilm stage at day 1, a significant part of the descendants of the primary colony formed colonies (i.e., microcolonies) by day 3.

Microcolony formation occurs via cell cluster migration and fusion. Further detailed time-lapse microscopy revealed that the small cell clusters that had formed subsequent to the dissolution of the primary colony moved along the surface and fused together in a self-organized manner to form microcolonies (Fig. 4; see also Movie S4 in the supplemental material). This dynamic self-reorganization of *Acinetobacter* sp. C6 cell clusters within the niche space resulted in an increasingly uniform pattern. Neighboring cell clusters moved either away or toward each other to fuse into microcolonies with ultimately relatively equal distances to each other (Fig. 1 and 4; see also Movie S4). Intriguingly, the cell clusters were able to move independently of the flow direction, indicating that in this particular stage the medium flow did not determine the processes of self-organization.

Spatial abundance distribution is dependent on historical contingency. The observations that only a fraction of cells form colonies (i.e., primary colonies) in the early biofilm stage but that many of the descendants of the primary colony form microcolonies in later stages indicated that phenotypic variants may have formed in the early biofilm stage. To explore this hypothesis, we isolated cells from microcolonies using a micromanipulator. There were no apparent differences between the variant cells isolated from microcolonies and the original cells of *Acinetobacter* sp. C6 used to inoculate the biofilm in terms of growth physiology in liquid medium or on agar plates. However, these cells exhibited hyper-microcolony formation when grown in flow chambers: Already within 12 to 15 h after flow chamber inoculation with variants, microcolonies developed throughout the niche space (see Fig. S4a in the supplemental material). Moreover, when we mixed and initiated biofilms with differentially tagged isogenic variant cells (1:1, Gfp-tagged cells plus Rfp-tagged cells), green and red microcolonies showed a random distribution and did not arrange in monochromatic clusters like the wild type (see Fig. S4b). This suggests that microcolonies of the variant developed by clonal development immediately following attachment to the surface, and no preceding primary colony formation was required as observed for the wild-type strain. When competing the wild-type

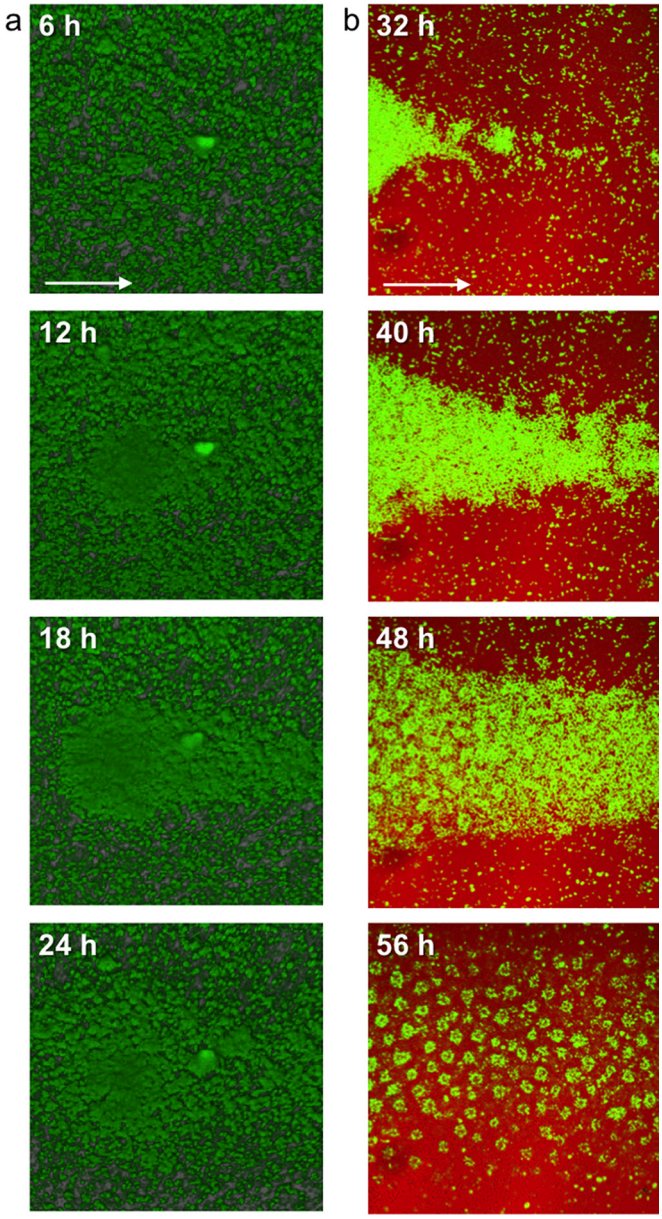

FIG 3 Primary colony formation and the emergence of cell clusters. Shown are confocal laser scanning micrographs of *Acinetobacter* sp. C6 grown in benzoate minimal medium at different time points. (a) Developmental stages of a primary colony after 6, 12, 18, and 24 h. (b) Developmental stages of emerging cell clusters downstream of the primary colony after 32, 40, 48, and 56 h. The flow direction is indicated by an arrow. Recordings of primary colony formation and emerging cell clusters are provided as Movies S1 to S3 in the supplemental material.

(Gfp) strain with the variant (Rfp) strain, the variant exhibited a higher degree of fitness, outcompeting the wild type already shortly after establishment in the flow chamber (see Fig. S4c). Moreover, the variant developed colonies also in glucose and citrate minimal media, in contrast to the wild type (see Fig. S4d). The apparent lack of variant formation in the wild type in the presence of glucose or citrate indicates that the occurrence of variants is impacted by environmental conditions.

Spatial abundance distribution is dependent on the order of events. The stability of the microcolony pattern formed by the variant strain raised the question of whether the microcolony pattern by the wild type is equally fixed (i.e., independent of environmentally conditions) or could be manipulated by targeted interventions, even after initiating development. We tested this question by performing two interventions. In the first intervention, *Acinetobacter* sp. C6 was cultivated for 2 days in the presence of benzoate and subsequently in the presence of glucose. In the second intervention, *Acinetobacter* sp. C6 was cultivated for 2 days in the presence of glucose and subsequently in the presence of benzoate. In the first case, microcolonies evolved and cells filled the previously unoccupied space subsequently (see Fig. S5a in the supplemental material). In the second case, cells distributed randomly across the entire niche space, and microcolonies evolved subsequently (Fig. S5b). In both cases, the final result was a niche

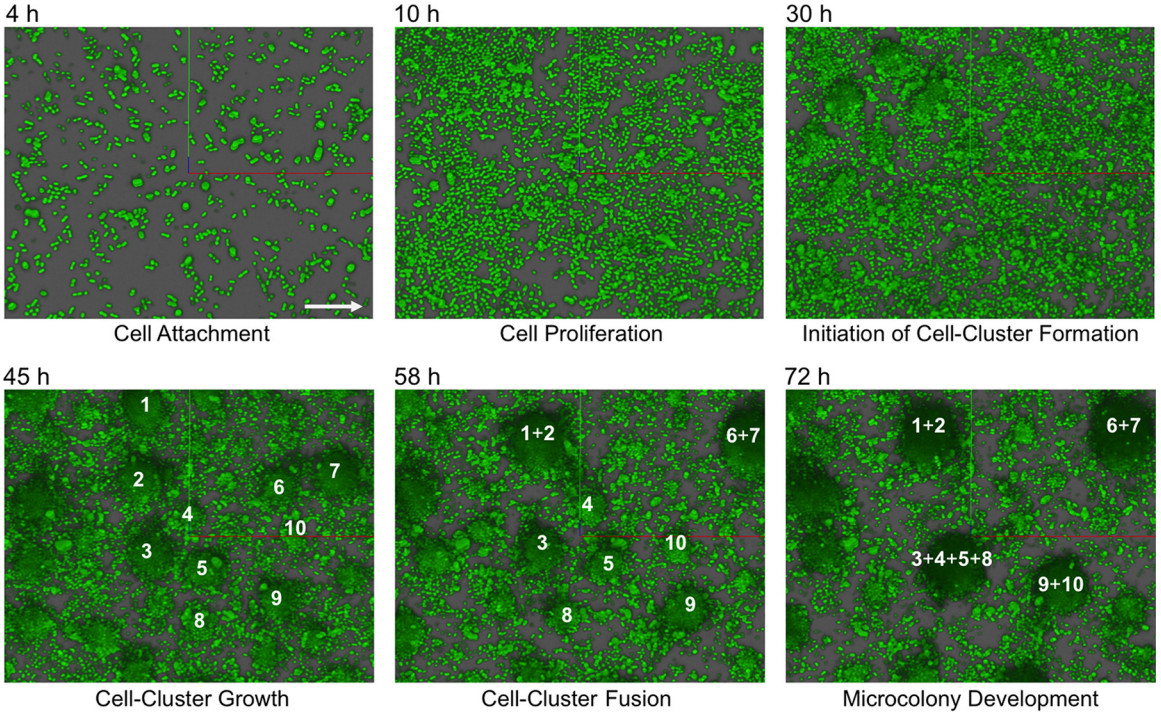

FIG 4 Microcolony formation occurs via cell cluster migration and fusion. Confocal laser scanning micrographs of *Acinetobacter* sp. C6 grown in benzoate minimal medium after 4, 10, 30, 45, 58, and 72 h indicate the formation and spatial organization of the cell clusters and their self-organized migration and fusion process. Individual cell clusters are numbered. The medium flow direction is indicated by an arrow. The individual micrographs are snapshots from a time series recording, which is available as Movie S4 in the supplemental material.

space that was occupied by microcolonies and cells colonizing the space in between them. However, microcolonies were dominating the spatial community structure in the case where cultivation was initiated by benzoate. This suggests that the initial short-term exposure had long-lasting effects and that spatial pattern development was influenced by the order of events.

Spatial distribution pattern by *Acinetobacter* sp. C6. In summary, the *Acinetobacter* sp. C6 microcolony pattern evolved in a reproducible order of events (Fig. 5). At day 1, cells were randomly distributed, and with increasing cell proliferation, large clonal primary colonies emerged. The large colonies were the result of the formation of phenotypic variants that consistently emerged in this early stage. At day 2, the primary colonies expanded to elongated patches by a combination of dissolution and cell reattachment downstream in flow direction, proliferation, and formation of small cell clusters. These cell clusters then rearranged via migration and fusion in a self-organized manner. The results by day 3 were evenly spaced microcolonies, leading to an overall uniform spatial distribution pattern.

DISCUSSION

Microbial communities exhibit distinct biogeographic patterns in nature as well as under laboratory conditions. *Acinetobacter* sp. C6 develops a microcolony pattern in flow chambers in the presence of aromates that serve as carbon and energy sources (references 9 and 20; also this study). Microcolony formation has been observed for a number of *Acinetobacter* species: in flow chambers in the presence of ethanol, attached to human epithelial and alveolar cells, and associated with dead *Candida albicans* filaments (24–26). Our ecological spatial pattern analysis revealed that *Acinetobacter* sp. C6 exhibited the tendency to form uniformly distributed microcolonies. This distribution pattern was reminiscent of biogeographic patterns observed in macroecology, like the uniform (evenly spaced) distributions described for the creosote desert bush (*Larrea* sp.) and colonies of stingless bees (*Trigonidae* sp.) (27, 28).

Ecological investigations on the spatial distribution of creosote desert shrubs revealed that their distribution patterns changed with growth (29). In early stages, small young shrubs exhibited a clumped distribution. As they grew to medium-sized shrubs, they tended to form a random distribution pattern. Finally, the large scrubs occurred in a regular pattern of evenly spaced individuals. Further investigations showed that young shrubs formed clumps because the seeds from which they emerged did not disperse far from the parent plant. Medium-sized shrubs exhibited a random distribution as some individuals died. With increasing growth, competition for nutrients increased, and consequently, shrubs maximized their distance to neighboring shrubs to reduce competitive pressure (29, 30). In *Acinetobacter* sp. C6, the microcolony pattern formation was dependent on the carbon source (see Fig. S2 and S5 in the supplemental material). Furthermore, the empty niche space in between microcolonies was characterized by oxygen depletion (9, 20) (see Fig. S3 in the supplemental material). Consequently, microcolonies maximized their distance to neighboring microcolonies in response to competition for oxygen. The intriguing cell cluster migration and fusion process at day 2 might have been induced by the decreasing oxygen concentration that coincides with increasing population size. As a result, the cell clusters moved in a "live or die" reaction and formed microcolonies,

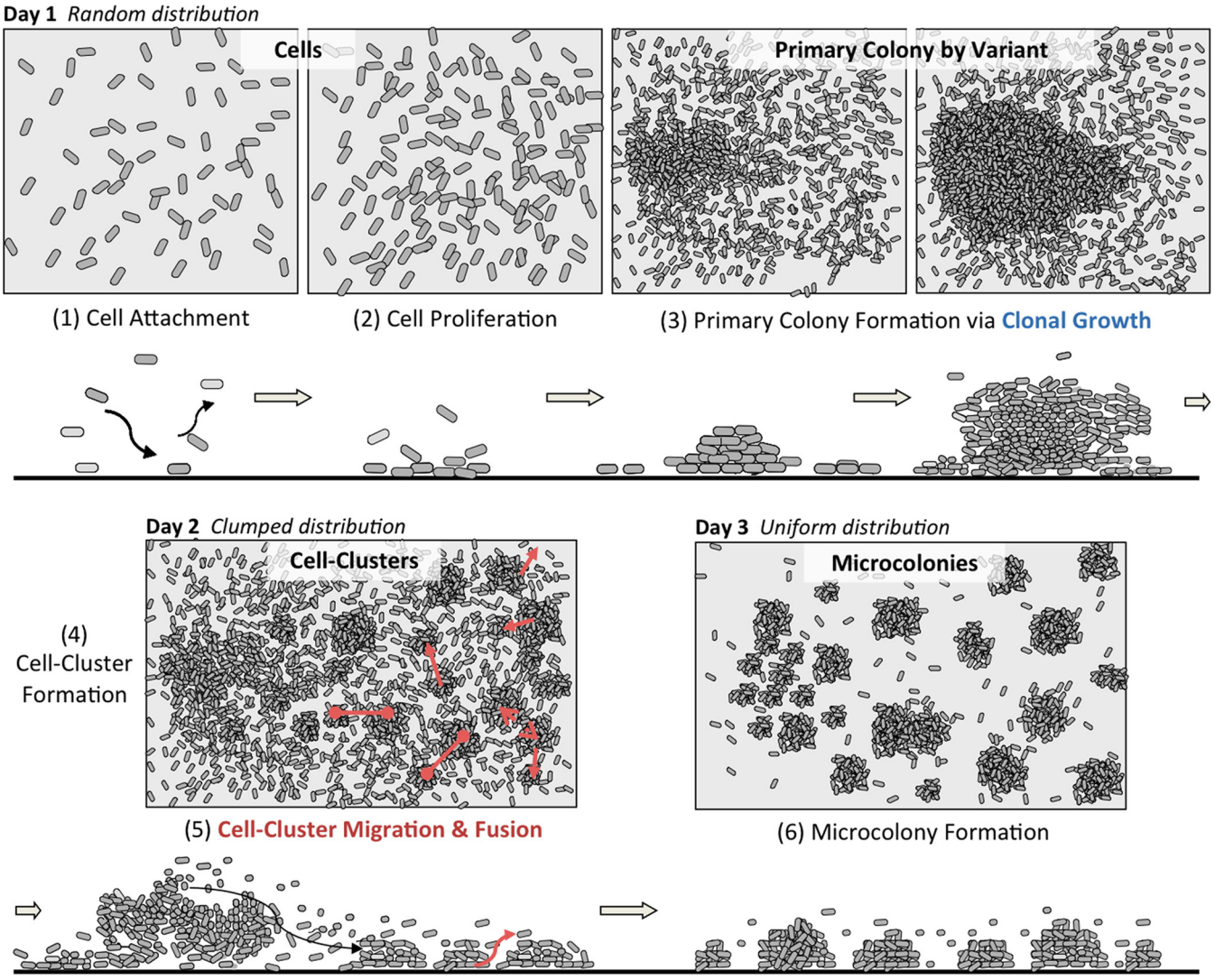

FIG 5 Schematic illustration of the spatial abundance distribution patterns by *Acinetobacter* sp. C6 when cultivated in the presence of aromates over 3 days. For a detailed description of the involved factors and processes, see the text.

which ultimately provide a larger surface area exposed to the surrounding environment containing oxygen.

The *Acinetobacter* sp. C6 microcolonies can also be interpreted as a clumped distribution of cells that form in response to patchy resources, as observed for phytoplankton or corals (31, 32). Once microcolonies have formed, though, they can be seen as individual, multicellular, biological units that maximize their distances to each other in response to competition for resources. Ecological theory predicts that individuals closer to each other experience competition, which can lead to a shift in their position along the niche axis, and individuals immigrate into communities via a self-organized process (33–35). The results are groups of coexisting individuals, arranging in evenly spaced entities that are functionally equivalent (neutral) (33–35).

The processes that lead to the transition from unicellular to multicellular life are poorly understood. Multicellularity in the microbial world is abundant and evident in filaments, fruiting bodies, and mycelial colonies (36–40). A requirement for the overall functioning of the multicellular entities is division of labor, which can emerge in response to different environmental conditions experienced at the microscale level within the multicellular unit. Division of labor, a consequence of cell differentiation, may also reduce effects of competition within the group and increase the fitness of the multicellular unit as a whole, as may be the case for *Acinetobacter* sp. C6. Furthermore, multicellularity can offer increased tolerance to environmental stress and improved access to resources (12, 40–42).

In the two-species consortium of *P. putida* and *Acinetobacter* sp. C6, the generated multicellular units of *Acinetobacter* sp. C6 provide an opportunity for *P. putida* to colonize the void nice space (9). *P. putida* variants evolve that have an increased ability to attach to the *Acinetobacter* sp. C6 microcolonies. This observation is in line with ecological theory that predicts that other species can occupy the void niche space between the self-organized groups of one species (34). *P. putida* increases in this way its access to benzoate, produced by *Acinetobacter* sp. C6, which it can utilize as a carbon and energy source. Hence, the present study reveals not only that *P. putida* developed variants and thereby improved its

interaction with *Acinetobacter* sp. C6 microcolonies but also that *Acinetobacter* sp. C6 forms variants to optimize its adaptation to the present niche. In fact, it appears that *P. putida* evolves variants in response to the formation of *Acinetobacter* sp. C6 variants that dominate the niche space in a characteristic pattern of microcolonies, to which *P. putida* variant cells then attach (9–11).

The *Acinetobacter* sp. C6 phenotypic variants may originate from one or several events related to bistability, phase variation, stochastic gene expression, spontaneous gene amplification, epigenetics, or mutation, similar to what has been described for other bacteria (9, 43–47). Addressing this aspect will require careful investigations at the single-cell level, as biofilms are traditionally initiated by a population of cells and one would need to follow the genotype and phenotype for each individual cell over several generations. For example, when the variant is introduced into flow chambers, it forms microcolonies earlier than does the wild type (see Fig. S4a in the supplemental material). However, it is unclear whether all cells introduced are identical and have an early-microcolony-formation phenotype or if only a fraction of introduced cells have this capability and outcompete other cells that may have a significantly reduced proliferation rate or possibly detached from the substratum.

Based on the present and previous studies, we conclude that the laboratory two-species consortium of *P. putida* and *Acinetobacter* sp. C6 exhibits features of coadaptation, resulting in a community that was more stable and more productive (9). By combining ecology and metabolic engineering, such communities may offer sustainable opportunities for enhancing the production of valuable chemicals in biotechnological settings, as well as improve processes in the bioremediation of toxic compounds (48).

ACKNOWLEDGMENTS

We thank Tove Johansen and Claus Sternberg for expert technical assistance.

This work was supported by a grant to Søren Molin from the Danish Research Council. Sünje J. Pamp was supported by a grant from Carlsbergfondet.

The authors declare no conflict of interest.

REFERENCES

1. **Martiny JBH, Bohannan BJM, Brown JH, Colwell RK, Fuhrman JA, Green JL, Horner-Devine MC, Kane M, Krumins JA, Kuske CR, Morin PJ, Naeem S, Øvreås L, Reysenbach A-L, Smith VH, Staley JT.** 2006. Microbial biogeography: putting microorganisms on the map. Nat Rev Microbiol **4:**102–112. http://dx.doi.org/10.1038/nrmicro1341.
2. **Besemer K, Hödl I, Singer G, Battin TJ.** 2009. Architectural differentiation reflects bacterial community structure in stream biofilms. ISME J **3:**1318–1324. http://dx.doi.org/10.1038/ismej.2009.73.
3. **Kolenbrander PE, Palmer RJ, Periasamy S, Jakubovics NS.** 2010. Oral multispecies biofilm development and the key role of cell-cell distance. Nat Rev Microbiol **8:**471–480. http://dx.doi.org/10.1038/nrmicro2381.
4. **Mukherjee S, Juottonen H, Siivonen P, Quesada CL, Tuomi P, Pulkkinen P, Yrjälä K.** 2014. Spatial patterns of microbial diversity and activity in an aged creosote-contaminated site. ISME J **8:**2131–2142. http://dx.doi.org/10.1038/ismej.2014.151.
5. **Wilmes P, Remis JP, Hwang M, Auer M, Thelen MP, Banfield JF.** 2009. Natural acidophilic biofilm communities reflect distinct organismal and functional organization. ISME J **3:**266–270. http://dx.doi.org/10.1038/ismej.2008.90.
6. **Fazli M, Bjarnsholt T, Kirketerp-Moller K, Jorgensen B, Andersen AS, Krogfelt KA, Givskov M, Tolker-Nielsen T.** 2009. Nonrandom distribution of Pseudomonas aeruginosa and Staphylococcus aureus in chronic wounds. J Clin Microbiol **47:**4084–4089. http://dx.doi.org/10.1128/JCM.01395-09.
7. **Blazejak A, Erseus C, Amann R, Dubilier N.** 2005. Coexistence of bacterial sulfide oxidizers, sulfate reducers, and spirochetes in a gutless worm (Oligochaeta) from the Peru Margin. Appl Environ Microbiol **71:**1553–1561. http://dx.doi.org/10.1128/AEM.71.3.1553-1561.2005.
8. **Nielsen AT, Tolker-Nielsen T, Barken KB, Molin S.** 2000. Role of commensal relationships on the spatial structure of a surface-attached microbial consortium. Environ Microbiol **2:**59–68. http://dx.doi.org/10.1046/j.1462-2920.2000.00084.x.
9. **Hansen SK, Rainey PB, Haagensen JAJ, Molin S.** 2007. Evolution of species interactions in a biofilm community. Nature **445:**533–536. http://dx.doi.org/10.1038/nature05514.
10. **Christensen BB, Sternberg C, Andersen JB, Eberl L, Møller S, Givskov M, Molin S.** 1998. Establishment of new genetic traits in a microbial biofilm community. Appl Environ Microbiol **64:**2247–2255.
11. **Christensen BB, Haagensen JAJ, Heydorn A, Molin S.** 2002. Metabolic commensalism and competition in a two-species microbial consortium. Appl Environ Microbiol **68:**2495–2502. http://dx.doi.org/10.1128/AEM.68.5.2495-2502.2002.
12. **Pamp SJ, Gjermansen M, Johansen HK, Tolker-Nielsen T.** 2008. Tolerance to the antimicrobial peptide colistin in Pseudomonas aeruginosa biofilms is linked to metabolically active cells, and depends on the pmr and mexAB-oprM genes. Mol Microbiol **68:**223–240. http://dx.doi.org/10.1111/j.1365-2958.2008.06152.x.
13. **Møller S, Pedersen AR, Poulsen LK, Arvin E, Molin S.** 1996. Activity and three-dimensional distribution of toluene-degrading Pseudomonas putida in a multispecies biofilm assessed by quantitative in situ hybridization and scanning confocal laser microscopy. Appl Environ Microbiol **62:**4632–4640.
14. **Haagensen JAJ, Hansen SK, Johansen T, Molin S.** 2002. In situ detection of horizontal transfer of mobile genetic elements. FEMS Microbiol Ecol **42:**261–268. http://dx.doi.org/10.1111/j.1574-6941.2002.tb01016.x.
15. **Sternberg C, Tolker-Nielsen T.** 2006. Growing and analyzing biofilms in flow cells. Curr Protoc Microbiol Chapter 1:Unit 1B.2. http://dx.doi.org/10.1002/9780471729259.mc01b02s00.
16. **Møller S, Sternberg C, Andersen JB, Christensen BB, Ramos JL, Givskov M, Molin S.** 1998. In situ gene expression in mixed-culture biofilms: evidence of metabolic interactions between community members. Appl Environ Microbiol **64:**721–732.
17. **Heydorn A, Nielsen AT, Hentzer M, Sternberg C, Givskov M, Ersboll BK, Molin S.** 2000. Quantification of biofilm structures by the novel computer program COMSTAT. Microbiology **146**(Part 10)**:**2395–2407.
18. **Schneider CA, Rasband WS, Eliceiri KW.** 2012. NIH Image to ImageJ: 25 years of image analysis. Nat Methods **9:**671–675. http://dx.doi.org/10.1038/nmeth.2089.
19. **Clark PJ, Evans FC.** 1954. Distance to nearest neighbor as a measure of spatial relationships in populations. Ecology **35:**445–453. http://dx.doi.org/10.2307/1931034.
20. **Hansen SK, Haagensen JAJ, Gjermansen M, Jorgensen TM, Tolker-Nielsen T, Molin S.** 2007. Characterization of a Pseudomonas putida rough variant evolved in a mixed-species biofilm with Acinetobacter sp. strain C6. J Bacteriol **189:**4932–4943. http://dx.doi.org/10.1128/JB.00041-07.
21. **Klausen M, Aaes-Jørgensen A, Molin S, Tolker-Nielsen T.** 2003. Involvement of bacterial migration in the development of complex multicellular structures in Pseudomonas aeruginosa biofilms. Mol Microbiol **50:**61–68. http://dx.doi.org/10.1046/j.1365-2958.2003.03677.x.
22. **Reisner A, Haagensen JAJ, Schembri MA, Zechner EL, Molin S.** 2003. Development and maturation of Escherichia coli K-12 biofilms. Mol Microbiol **48:**933–946. http://dx.doi.org/10.1046/j.1365-2958.2003.03490.x.
23. **Pamp SJ, Tolker-Nielsen T.** 2007. Multiple roles of biosurfactants in structural biofilm development by Pseudomonas aeruginosa. J Bacteriol **189:**2531–2539. http://dx.doi.org/10.1128/JB.01515-06.
24. **Gaddy JA, Actis LA.** 2009. Regulation of Acinetobacter baumannii biofilm formation. Future Microbiol **4:**273–278. http://dx.doi.org/10.2217/fmb.09.5.
25. **de Breij A, Haisma EM, Rietveld M, El Ghalbzouri A, van den Broek PJ, Dijkshoorn L, Nibbering PH.** 2012. Three-dimensional human skin equivalent as a tool to study Acinetobacter baumannii colonization. Antimicrob Agents Chemother **56:**2459–2464. http://dx.doi.org/10.1128/AAC.05975-11.
26. **James GA, Korber DR, Caldwell DE, Costerton JW.** 1995. Digital image analysis of growth and starvation responses of a surface-colonizing Acinetobacter sp. J Bacteriol **177:**907–915.

27. **Shreve F.** 1942. The desert vegetation of North America. Bot Rev **8:**195–246. http://dx.doi.org/10.1007/BF02882228.
28. **Hubbell PS, Johnson LK.** 1977. Competition and nest spacing in a tropical stingless bee community. Ecology **58:**949–963. http://dx.doi.org/10.2307/1936917.
29. **Phillips DL, MacMahon JA.** 1981. Competition and spacing patterns in desert shrubs. J Ecol **69:**97–115. http://dx.doi.org/10.2307/2259818.
30. **Brisson J, Reynolds JF.** 1994. The effect of neighbors on root distribution in a creosotebush (Larrea Tridentata) population. Ecology **75:**1693–1702. http://dx.doi.org/10.2307/1939629.
31. **Segura AM, Calliari D, Kruk C, Conde D, Bonilla S, Fort H.** 2011. Emergent neutrality drives phytoplankton species coexistence. Proc R Soc B Biol Sci **278:**2355–2361. http://dx.doi.org/10.1098/rspb.2010.2464.
32. **Dornelas M, Connolly SR.** 2008. Multiple modes in a coral species abundance distribution. Ecol Lett **11:**1008–1016. http://dx.doi.org/10.1111/j.1461-0248.2008.01208.x.
33. **Matthews TJ, Whittaker RJ.** 2014. Neutral theory and the species abundance distribution: recent developments and prospects for unifying niche and neutral perspectives. Ecol Evol **4:**2263–2277. http://dx.doi.org/10.1002/ece3.1092.
34. **Vergnon R, van Nes EH, Scheffer M.** 2012. Emergent neutrality leads to multimodal species abundance distributions. Nat Commun **3:**663–666. http://dx.doi.org/10.1038/ncomms1663.
35. **Barabás G, D'Andrea R, Rael R, Meszéna G, Ostling A.** 2013. Emergent neutrality or hidden niches? Oikos **122:**1565–1572. http://dx.doi.org/10.1111/j.1600-0706.2013.00298.x.
36. **Chater KF.** 1993. Genetics of differentiation in Streptomyces. Annu Rev Microbiol **47:**685–713. http://dx.doi.org/10.1146/annurev.mi.47.100193.003345.
37. **Pamp SJ, Harrington ED, Quake SR, Relman DA, Blainey PC.** 2012. Single-cell sequencing provides clues about the host interactions of segmented filamentous bacteria (SFB). Genome Res **22:**1107–1119. http://dx.doi.org/10.1101/gr.131482.111.
38. **Kaiser D.** 2003. Coupling cell movement to multicellular development in myxobacteria. Nat Rev Microbiol **1:**45–54. http://dx.doi.org/10.1038/nrmicro733.
39. **Flores E, Herrero A.** 2010. Compartmentalized function through cell differentiation in filamentous cyanobacteria. Nat Rev Microbiol **8:**39–50. http://dx.doi.org/10.1038/nrmicro2242.
40. **Shapiro JA.** 1998. Thinking about bacterial populations as multicellular organisms. Annu Rev Microbiol **52:**81–104. http://dx.doi.org/10.1146/annurev.micro.52.1.81.
41. **Rainey PB.** 2007. Unity from conflict. Nature **446:**616. http://dx.doi.org/10.1038/446616a.
42. **Khare A, Shaulsky G.** 2006. First among equals: competition between genetically identical cells. Nat Rev Genet **7:**577–583. http://dx.doi.org/10.1038/nrg1875.
43. **Cárcamo-Oyarce G, Lumjiaktase P, Kümmerli R, Eberl L.** 2015. Quorum sensing triggers the stochastic escape of individual cells from Pseudomonas putida biofilms. Nat Commun **6:**1–9. http://dx.doi.org/10.1038/ncomms6945.
44. **van der Woude MW.** 2011. Phase variation: how to create and coordinate population diversity. Curr Opin Microbiol **14:**205–211. http://dx.doi.org/10.1016/j.mib.2011.01.002.
45. **Kærn M, Elston TC, Blake WJ, Collins JJ.** 2005. Stochasticity in gene expression: from theories to phenotypes. Nat Rev Genet **6:**451–464. http://dx.doi.org/10.1038/nrg1615.
46. **Anderson RP, Roth JR.** 1977. Tandem genetic duplications in phage and bacteria. Annu Rev Microbiol **31:**473–505. http://dx.doi.org/10.1146/annurev.mi.31.100177.002353.
47. **Veening J-W, Smits WK, Kuipers OP.** 2008. Bistability, epigenetics, and bet-hedging in bacteria. Annu Rev Microbiol **62:**193–210. http://dx.doi.org/10.1146/annurev.micro.62.081307.163002.
48. **Jagmann N, Philipp B.** 2014. Design of synthetic microbial communities for biotechnological production processes. J Biotechnol **184:**209–218. http://dx.doi.org/10.1016/j.jbiotec.2014.05.019.